

# High-resolution, topobathymetric LiDAR coastal zone characterisation

An article by FRANK STEINBACHER, RAMONA BARAN, MIKKEL S. ANDERSEN, ZYAD AL-HAMDANI, LAURIDS R. LARSEN, MARTIN PFENNIGBAUER and VERNER B. ERNSTSEN

Coastal and tidal environments are valuable ecosystems, which, however, are under pressure in many areas around the world due to globalisation and/or climate change. Detailed mapping of these environments is required in order to manage the coastal zone in a sustainable way. However, historically these transition zones between land and water are difficult or even impossible to map and investigate in high spatial resolution due to the challenging environmental conditions. The new generation of airborne topobathymetric light detection and ranging (LiDAR) potentially enables full-coverage and high-resolution mapping of these land-water transition zones. We have carried out topobathymetric LiDAR surveys in the Knudedyb tidal inlet system in the Danish Wadden Sea and the Rødsand lagoon connected to Fehmarnbelt. Here, we present the preliminary results of these two surveys which were carried out at two locations with different environmental settings. We demonstrate the potential of using airborne

topobathymetric LiDAR for seamless mapping of land-water transition zones in challenging coastal environments, e.g. in an environment with high water column turbidity and continuously varying water levels due to tides as well as in an environment characterised by a very heterogeneous surface sediment composition.

topobathymetry | LiDAR | coastal zone | HydroVISH | point cloud classification

## 1 Introduction

Coastal and tidal environments are valuable ecosystems, which are highly impacted by globalisation, climate change, and human encroachment in many areas around the world. Detailed mapping of these environments is required in order to manage the coastal zone in an economically sustainable manner, but traditionally used methods are not sufficient to gain full coverage, comprehensive and high-resolution spatial data of these shallow water areas (e.g., Steinbacher et al. 2013; Dobler et al. 2013). This is particularly due to highly variable environmental conditions of the land-water transition zone impeding an efficient monitoring. Furthermore, the results often have a very low spatial resolution, are expensive and time consuming. In contrast, by using a new generation of laser scanning equipment (green wavelength 532 nm)

airborne topobathymetric laser scanning can provide measurements of the land surface and the river bed or seabed within a single measurement process (Fig. 1). The measurements have both a very high accuracy ( $\pm$  centimetres) and a very high resolution (about 20 to 30 points/m<sup>2</sup>) (Andersen et al. 2016). Contrary to previous methods, which are mostly cross-section/profile based or only consider subareas, the comprehensive spatial information gained by the new LiDAR technique signifies an enormous and game changing advancement in the recording of underwater information. Among other factors the penetration depth of the laser beam crucially depends on the turbidity of the water body. At ideal viewing conditions, the sea/river bed can be detected down to about 10 to 11 m depth.

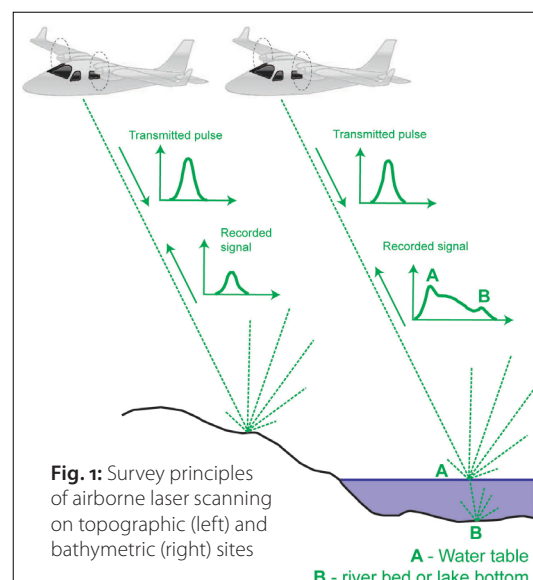
Thus, we performed topobathymetric LiDAR surveys in the Knudedyb tidal inlet system, a coastal environment in the Danish Wadden Sea which is part of the Wadden Sea National Park and UNESCO World Heritage, and in the Rødsand lagoon, which is a NATURA2000 site located in close vicinity of the planned Fehmarnbelt fixed link (for locations Fig. 2 and 3). These two surveys were conducted in order to:

- Derive characteristic properties of the morphology, surface sediment, the vegetation and the water column in land-water transition zones like rivers, lakes, wetlands, estuaries and coasts;
- Improve the understanding of the dynamics of these properties in shallow water ecosystems, which are under pressure due to changing environmental conditions driven by climate change;
- Develop tools for quantifying geological resources, habitat distributions and system-indicators in land-water transition zones, developed

## Authors

Frank Steinbacher and Ramona Baran work for Airborne HydroMapping GmbH in Innsbruck, Austria. Mikkel S. Andersen and Verner B. Ernstsen are from the Department of Geosciences and Natural Resource Management, University of Copenhagen, Denmark. Ziad Al-Hamdani is from the Geological Survey of Denmark and Greenland (GEUS), Copenhagen, Denmark. Laurids R. Larsen works for NIRAS in Allerød, Denmark. Martin Pfennigbauer is from RIEGL Laser Measurement Systems GmbH in Horn, Austria.

info@ahm.co.at



in and for a GIS in order to optimise application by end-users.

## 2 Project sites and airborne survey

The Knudedyb tidal inlet system is located at the west coast of Denmark in the Danish Wadden Sea, and is part of the Wadden Sea National Park and belongs to the UNESCO World Heritage (Fig. 2). The coastal area is strongly influenced by tides with a mean tidal range of 1.6 m (Pedersen and Bartholdy 2006), and is characterised by a manifold environment in terms of biodiversity, geodiversity, and complexity of coastal processes (sediment transport and morphologic changes). The Knudedyb site was surveyed two times on 19 April 2014 and 30 May 2014 at low tide under clear weather conditions and offshore winds using the VQ820G sensor (RIEGL LMS; Fig. 2). About 118 scan strips were acquired during both surveys: 37 strips in the first run and 81 strips in the second. The strips were adjusted with respect to each other to derive an internally consistent point cloud (internal accuracy of 6 to 10 cm given as standard deviation). Subsequently, the point cloud was georeferenced to terrestrially measured reference planes (accuracy of 4 to 9 cm given as standard deviation).

The Rødsand lagoon is located at the south coast of Lolland and is connected to the Fehmarnbelt; it is a NATURA2000 site located in close vicinity of the planned Fehmarnbelt fixed link (Fig. 3). The lagoon is approximately 30 × 8.5 km wide. In the offshore area near the lagoon two offshore wind parks are established (Rødsand 1 & 2). The lagoon is bordered by a broad sand barrier at its southern edge extending from Gedser in the east towards the west, intersected by three inlets. This sand barrier plus several N-S traverses across the Rødsand lagoon were surveyed on 7 September 2015 at clear and relatively calm water conditions as well as clear weather using the VQ880G sensor (RIEGL LMS; Fig. 3 and 4). In total, 35 scan strips were acquired yielding 70 single strips due to simultaneous forward and backward recording of the VQ880G. The strips were adjusted to each other to gain an internally consistent point cloud similar to the Knudedyb tidal inlet data (internal accuracy of ca. 5 cm given as standard deviation).

## 3 Point cloud processing using HydroVISH

### 3.1 Noise filtering

The further point cloud processing of the topobathymetric LIDAR data was done using the HydroVISH software package developed by AHM. Prior to point cloud classification, flaw echoes (noise) need to be removed from the raw point cloud (Fig. 5). These echoes were recorded because the sensor setting was extremely sensitive in order to capture as many echoes from the water surface as well as achieving a best possible penetration. For each point of the point cloud, the point density within a 0.75 m radius was evaluated and a point

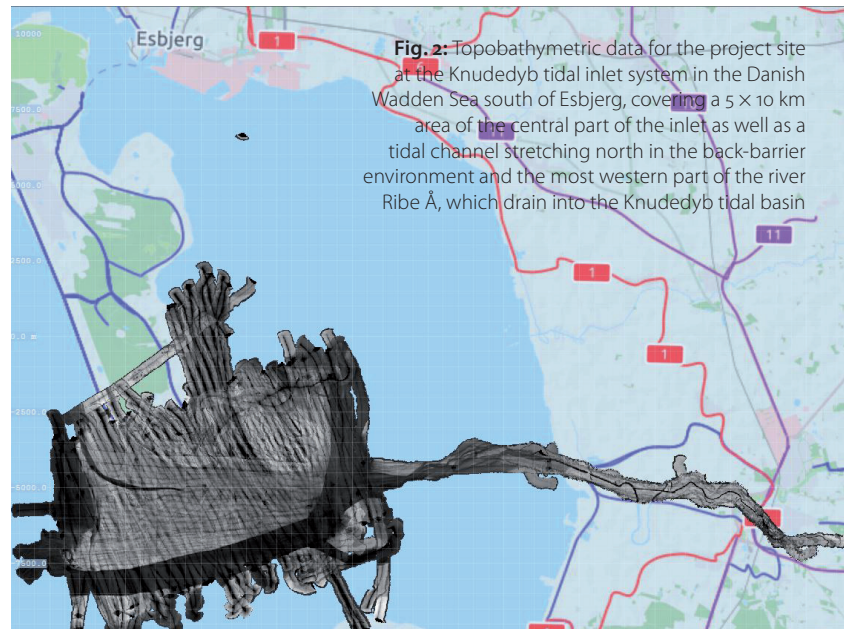
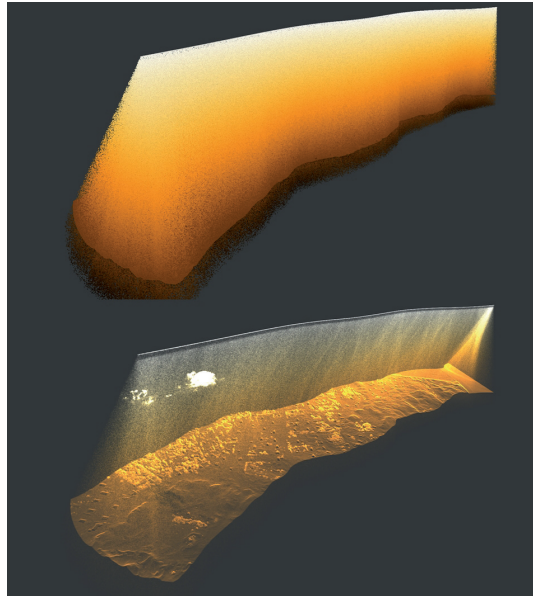


**Fig. 5:** Flaw echoes for a scan strip from the Knudedyb tidal inlet system



**References**

Andersen, Mikkel S.; A. Gergely; Ziad Al-Hamdani; Frank Steinbacher; Laurids R. Larsen; Verner B. Ernstsen (2016): Processing and accuracy of topobathymetric LiDAR data in land-water transition zones; *Hydrology and Earth System Sciences*, doi:10.5194/hess-2016-3, in review

Dobler, Wolfgang; Ramona Baran; Frank Steinbacher; Marcel Ritter; Manfred Niederwieser; Werner Bengler; Markus Aufleger (2013): Die Verbindung moderner und klassischer Gewässervermessung; *Hydrographische Nachrichten*, HN 95, pp. 16–22

Mandlbürger Gottfried; Martin Pfennigbauer; Norbert Pfeifer (2013): Analyzing near water surface penetration in laser bathymetry – a case study at the river Pielach; *ISPRS Annals of the Photogrammetry, Remote Sensing and Spatial Information Sciences*, Volume II-5/W2, pp. 175–180

Pedersen, J. B. T.; Jesper Bartholdy (2006): Budgets for fine-grained sediment in the Danish Wadden Sea; *Marine Geology*, 235, pp. 101–117

Steinbacher, Frank; Ramona Baran; Wolfgang Dobler; Markus Aufleger; Lutz Christiansen (2013): Combining Novel and Traditional Survey Technologies to Monitor Coastal Environments: Airborne Hydromapping and Sonar Data along the Baltic Sea Coastline, Schleswig-Holstein, Germany; in: *Proceedings of the 35th IAHR World Congress*, Tsinghua University Press, Beijing

was identified as flaw echo, if the number of point neighbours was less than five within the given radius. The cleaned point cloud was subsequently classified.

**3.2 Point cloud classification**

First of all, the point cloud was mapped onto a 0.5 × 0.5 m grid using the deepest point per grid cell to classify terrain (terrain on land and water ground), and the highest point per grid cell to classify the rest (water body, buildings, vegetation). The differentiation among the two follows a height- and slope criterion. By intersecting the two grid data sets, the water land boundary was approximated. After manual correction of the raster classification, all rest raster points located within the water-land boundary are classified as water body including water surface, and all terrain raster points located within the water-land boundary are classified as water ground. The results of the raster classification are then transferred to the point cloud and controlled manually.

**3.3 Water surface model and refraction**

The laser beam is reflected and refracted at the boundary between air and water. The fact that light is about 25 % slower in water than in air ( $c_{air} = 299,710 \text{ km/s}$ ,  $c_{water} = 225,000 \text{ km/s}$ ) requires the application of a refraction- and runtime correction for all measurement points located below the water surface. Therefore, the water surface needs to be modelled based on all classified water-surface points. Those spread over a 20 to 30 cm thick band around the true water table and only the uppermost points (99 % quantile) were considered as valid points to model the actual water surface (Mandlbürger et al. 2013). The water-surface model was defined by element sizes of 1.5 m to 5 m, where the centre of each grid cell had the elevation  $z = q_{0.99}$ . The raster points were triangulated for the final water-surface model, which was then extrapolated towards the water-land boundary.

For applying the refraction correction three data sets are required: the point cloud with time stamp for each measurement point, the trajectory with time stamp for each point of the trajectory and the triangulated water-surface model. First of all, a pair of points with the same time stamp (P from the trajectory, and Q from the point cloud) and the vector between these two points was evaluated to determine the point, where the beam P-Q intersects the water surface S (Fig. 6). Therefore, the beam’s entering angle can be determined in order to correct the beam with respect to the refraction angle. Moreover, the beam’s length S-Q below water can be calculated in order to apply the runtime correction with respect to the refraction index. Using a refraction index of 1.33 for water and 1.000292 for air, the runtime correction was derived by:

$$\begin{aligned} & \text{Beam length under water unrefracted} \\ & \times (1/\text{refraction index water}) \\ & = \text{Beam length under water refracted.} \end{aligned}$$

The angle correction was calculated according the Snell’s refraction law:

$$\begin{aligned} & \text{Refraction index air} \\ & \times \sin(\text{angle between beam in air and water surface}) \\ & = \text{Refraction index water} \\ & \times \sin(\text{angle between water surface and beam in water}). \end{aligned}$$

The difference prior and after application of the refraction and runtime correction is shown in Fig. 7 for an exemplary cross-section. Corrected water-ground points (in blue) are located above their original position (in red). Terrain points above the water surface are not affected by this correction.

**Fig. 6:** Schematic illustration for refraction calculation

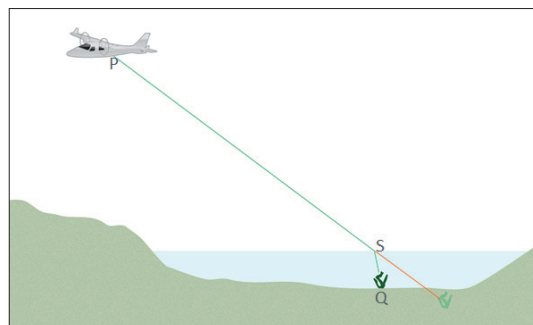
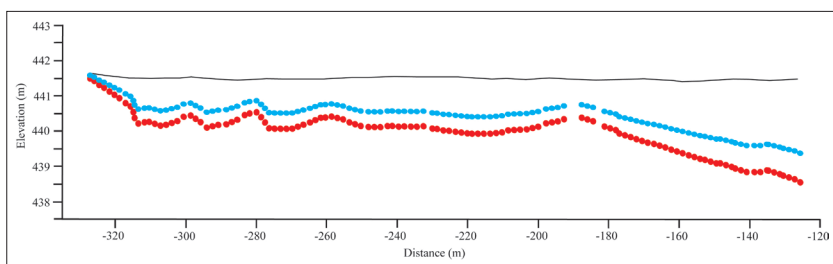


**Fig. 7:** Simplified cross-section to illustrate location of points prior (red) and after (blue) applying the refraction. Water table is marked in black



**3.3 Digital terrain modelling**

Finally, in order to generate high-resolution digital terrain models (DTMs) for both project sites the classified terrain points were mapped onto a 0.5 × 0.5 m grid using the mean elevation of all terrain points per grid cell (compare with Fig. 8). The DTMs serve as base for detailed mapping purposes.

es as well as morphologic analysis and comparison with terrestrially measured data.

#### 4 Preliminary results and discussion

Based on object detection Andersen et al. (2016) have demonstrated that the vertical accuracy and precision of the LiDAR data on land was  $\pm 8$  cm with a 95% confidence level; while the vertical precision below the water surface was  $\pm 4$  cm. Andersen et al. (2016) determined the horizontal mean error to  $\pm 10$  cm. Hence, the overall vertical and horizontal precision is within sub-decimetres scale. The same objects, a cement block ( $250 \times 125 \times 80$  cm) located on land as well as a steel frame ( $92 \times 92 \times 30$  cm) positioned in a shallow water area (Fig. 9), were also used to assess the feature-scale detection. The two objects, which were clearly visible in the point cloud, were modelled based on different approaches (triangulation vs. grid) and subsequently detailed morphological analysis (slope, etc.; Fig. 10) were conducted. The results indicate that such sharp-edged, sharp-cornered, and steep-angled features are smoothed, e.g. underestimation of slope angles (Fig. 10). This smoothing is mostly due to the footprint size of the topobathymetric LiDAR system (about 40 cm). Nevertheless, decimetre-scale features are well detected by airborne LiDAR topobathymetry. Hence, the preliminary results demonstrate that airborne topobathymetric LiDAR is a valuable tool to bridge land and water environments as well as to bridge morphological scales, thereby closing the gaps between terrestrial and marine surveys and between the mapping of individual morphological features and complete landscapes.

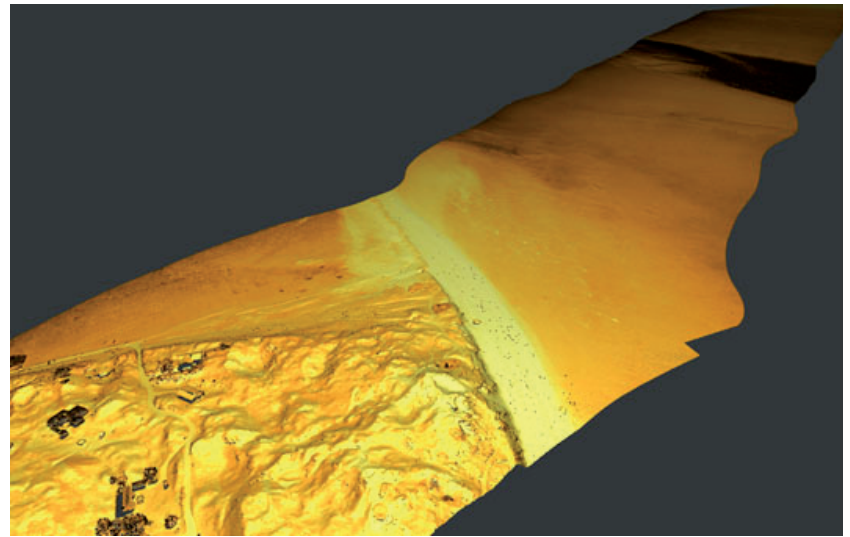


**Fig. 8:** DTM section from the Knudedyb tidal inlet system showing the complex and manifold morphologic patterns

#### 5 Conclusions

The results of our study underpin that topobathymetric surveying is a highly efficient and valuable tool for monitoring complex coastal areas. In tidal influenced areas with extremely variable water surface conditions, the seabed can be well detected at low tide down to depths of about 3 to 4 m (Knudedyb site), whereas in calm and clear water conditions within the Rød-sand lagoon the seabed was detected down to depths of 6 to 7 m. Moreover, small scale under-water features (decimetre- to metre-scale) can be readily identified in the data allowing detailed and area-based analysis of sediment transport and morphologic changes and to evaluate specific habitat characteristics and distribution. [↕](#)

**Fig. 9:** Small-scale objects at Knudedyb project site. Both objects are visible in the point cloud and are modelled based on triangulation and rasterisation

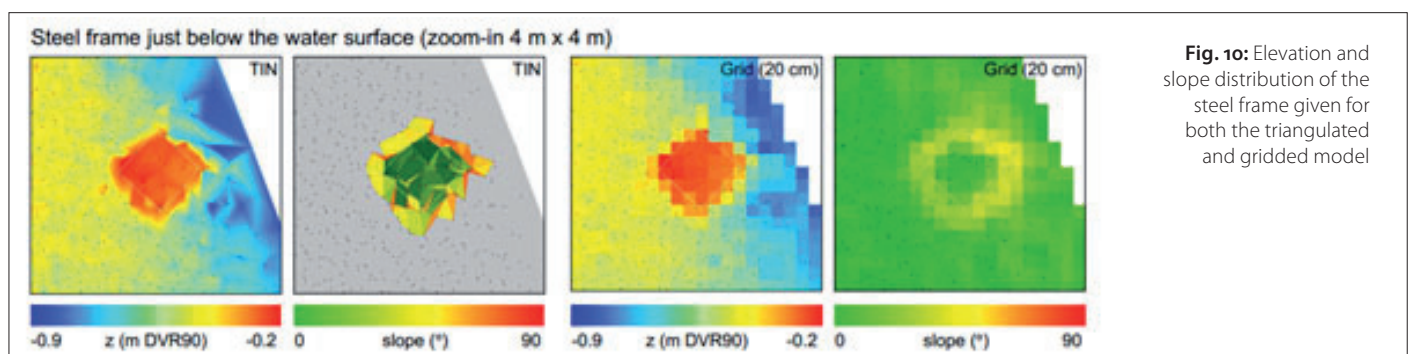
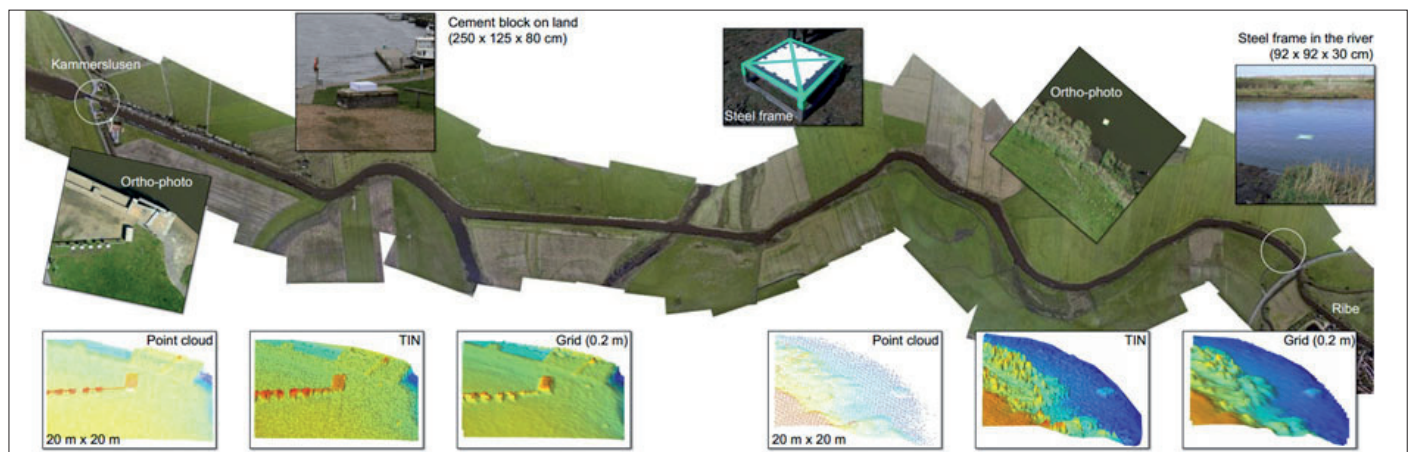


**Fig. 10:** Elevation and slope distribution of the steel frame given for both the triangulated and gridded model